Monthly Notices
of the
ROYAL ASTRONOMICAL SOCIETY

MNRAS **438,** 2413–2425 (2014)
Advance Access publication 2014 January 16

doi:10.1093/mnras/stt2360

Stellar diameters and temperatures – V. 11 newly characterized exoplanet host stars

Kaspar von Braun,[1,2]★ Tabetha S. Boyajian,[3] Gerard T. van Belle,[4] Stephen R. Kane,[5] Jeremy Jones,[6] Chris Farrington,[7] Gail Schaefer,[7] Norm Vargas,[7] Nic Scott,[7] Theo A. ten Brummelaar,[7] Miranda Kephart,[3] Douglas R. Gies,[6] David R. Ciardi,[8] Mercedes López-Morales,[9] Cassidy Mazingue,[2] Harold A. McAlister,[7] Stephen Ridgway,[10] P. J. Goldfinger,[7] Nils H. Turner[7] and Laszlo Sturmann[7]

[1]*Max-Planck-Institute for Astronomy (MPIA), Königstuhl 17, D-69117 Heidelberg, Germany*
[2]*Mirasol Institute, D-81679 Munich, Germany*
[3]*Yale University, New Haven, CT 06520-8101, USA*
[4]*Lowell Observatory, Flagstaff, AZ 86001 USA*
[5]*Department of Physics and Astronomy, San Francisco State University, 1600 Holloway Ave., San Francisco, CA 94132, USA*
[6]*Center for High Angular Resolution Astronomy and Department of Physics and Astronomy, Georgia State University, PO Box 5060, Atlanta, GA 30302-4106, USA*
[7]*The CHARA Array, Mount Wilson Observatory, Mount Wilson, CA 91023, USA*
[8]*NASA Exoplanet Science Institute, California Institute of Technology, MC 100-22, Pasadena, CA 91125, USA*
[9]*CfA, Cambridge, MA 02138, USA*
[10]*NOAO, Tucson, AZ 85719, USA*

Accepted 2013 December 3. Received 2013 November 21; in original form 2013 September 13

ABSTRACT

We use near-infrared interferometric data coupled with trigonometric parallax values and spectral energy distribution fitting to directly determine stellar radii, effective temperatures and luminosities for the exoplanet host stars 61 Vir, ρ CrB, GJ 176, GJ 614, GJ 649, GJ 876, HD 1461, HD 7924, HD 33564, HD 107383 and HD 210702. Three of these targets are M dwarfs. Statistical uncertainties in the stellar radii and effective temperatures range from 0.5 to 5 per cent and from 0.2 to 2 per cent, respectively. For eight of these targets, this work presents the first directly determined values of radius and temperature; for the other three, we provide updates to their properties. The stellar fundamental parameters are used to estimate stellar mass and calculate the location and extent of each system's circumstellar habitable zone. Two of these systems have planets that spend at least parts of their respective orbits in the system habitable zone: two of GJ 876's four planets and the planet that orbits HD 33564. We find that our value for GJ 876's stellar radius is more than 20 per cent larger than previous estimates and frequently used values in the astronomical literature.

Key words: techniques: interferometric – stars: fundamental parameters – stars: general – stars: late-type – planetary systems – infrared: stars.

1 INTRODUCTION

In the characterization of exoplanetary systems, knowledge of particularly the stellar radius and temperature are of paramount importance as they define the radiation environment in which the planets reside, and they enable the calculation of the circumstellar habitable zone's (HZ) location and boundaries. Furthermore, the radii and densities of any transiting exoplanets, which provide the deepest insights into planet properties, such as exoatmospheric studies or the studies of planetary interior structures, are direct functions of the radius and mass of the respective parent star. Recent advances in

★ E-mail: braun@mpia.de

sensitivity and angular resolution in long-baseline interferometry at wavelengths in the near-infrared and optical range have made it possible to circumvent assumptions of stellar radius by enabling direct measurements of stellar radius and other astrophysical properties for nearby, bright stars (e.g. Baines et al. 2008a,b, 2009, 2010; van Belle & von Braun 2009; von Braun et al. 2011a,b, 2012; Boyajian et al. 2012a,b, 2013; Huber et al. 2012, and references therein).

In this paper, we present interferometric observations (Section 2.1) that, in combination with trigonometric parallax values, produce directly determined stellar radii for 11 exoplanet host stars,[1] along with estimates of their stellar effective temperatures based on literature photometry (Section 3). We use these empirical stellar parameters to calculate stellar masses/ages where possible, and the locations and boundaries of the system HZs (Section 3.2). We discuss the implications for all the individual systems in Section 4 and conclude in Section 5.

2 DATA

In order to be as empirical as possible in the calculation of the stellar parameters of our targets, we rely on our interferometric observations to obtain angular diameters (Section 2.1), and we fit empirical spectral templates to literature photometry to obtain bolometric flux values (Section 2.2).

2.1 Interferometric observations

Our observational methods and strategy are described in detail in section 2.1 of Boyajian et al. (2013). We repeat aspects specific to the observations of the individual targets below.

The Georgia State University Center for High Angular Resolution Astronomy (CHARA) Array (ten Brummelaar et al. 2005) was used to collect our interferometric observations of exoplanet hosts in J, H and K' bands with the CHARA Classic beam combiner in single-baseline mode. The data were taken between 2010 and 2013 in parallel with our interferometric survey of main-sequence stars (Boyajian et al. 2012b, 2013). Our requirement that any target be observed on at least two nights with at least two different baselines serves to eliminate or reduce systematic effects in the observational results (von Braun et al. 2012; Boyajian et al. 2013). We note that were not able to adhere this strategy for HD 107383, which was only observed during one night due to weather constraints during the observing run.

An additional measure to reduce the influence of systematics is the alternating between multiple interferometric calibrators during observations to eliminate effects of atmospheric and instrumental systematics. Calibrators, whose angular sizes are estimated using size estimates from the Jean-Marie Mariotti Center Catalogue at http://www.jmmc.fr/searchcal (Bonneau et al. 2006, 2011; Lafrasse et al. 2010a,b), are chosen to be small sources of similar brightness as, and small angular distance to, the respective target. A log of the interferometric observations can be found in Table 1.[2]

The uniform disc and limb-darkened angular diameters ($\theta_{\rm UD}$ and $\theta_{\rm LD}$, respectively; see Table 2) are found by fitting the calibrated visibility measurements (Figs 1 and 2) to the respective functions for each relation.[3] These functions may be described as nth-order Bessel functions that are dependent on the angular diameter of the star, the projected distance between the two telescopes

Table 1. Log of interferometric observations.

Star UT date	Baseline	No. of Obs (filter)	Calibrators
61 Vir			
2012-04-09	W1/E1	13(H)	HD 113289, HD 116928
2012-04-10	S1/E1	3(H)	HD 113289, HD 116928
ρ CrB			
2013-05-03	S1/E1	4(H)2(K')	HD 139389, HD 149890
2013-08-18	S1/W1	3(H)	HD 139389, HD 146946
GJ 176			
2010-09-16	W1/E1	7(H)	HD 29225, HD 27524
2010-09-17	W1/E1	2(H)	HD 27534
2010-09-20	S1/E1	4(H)	HD 29225
2010-11-10	W1/E1	3(H)	HD 29225
GJ 614[a]			
2010-06-28	W1/E1	10(H)	HD 144579, HD 142908
2010-06-29	W1/E1	6(H)	HD 144579, HD 142908
2010-09-18	S1/E1	4(H)	HD 144579
GJ 649			
2010-06-29	W1/E1	5(H)	HD 153897
2010-06-30	S1/E1	6(H)	HD 153897, HD150205
2010-07-01	S1/E1	7(H)	HD 153897, HD150205
GJ 876			
2011-08-17	S1/E1	11(H)	HD 215874, HD 217681
2011-08-18	S1/E1	10(H)	HD 215874, HD 217681
2011-08-19	W1/E1	6(H)	HD 215874, HD 216402
2011-08-20	W1/E1	6(H)	HD 217861, HD 216402
HD 1461			
2011-08-22	S1/E1	7(H)	HD 966, HD 1100
2011-10-03	S1/E1	7(H)	HD 966, HD 1100
2013-08-17	E1/W1	5(H)	HD 966, HD 1100
HD 7924			
2010-09-17	W1/E1	9(H)	HD 9407, HD 6798
2011-08-21	W1/S1	6(H)	HD 9407, HD 6798
HD 33564			
2010-09-16	W1/E1	2(H)	HD 29329
2010-09-17	W1/E1	1(H)	HD 62613
2010-11-10	W1/E1	9(H)	HD 36768, HD 46588
2013-08-16	S1/W1	3(H)	HD 29329, HD 62613
2013-08-17	S1/W1	1(H)	HD 29329, HD 36768, HD 46588
HD 107383			
2013-05-06	E2/W2	3(H)	HD 106661, HD 108468
2013-05-06	S2/W2	4(H)	HD 106661, HD 104452
HD 210702			
2013-08-18	S1/E1	5(H)1(J)	HD 210074, HD 206043
2013-08-19	E1/W1	2(H)	HD 210074, HD 206043
2013-08-22	E1/W1	7(H)	HD 210074, HD 207223
2013-08-22	S1/E1	1(J)	HD 210074, HD 207223

[a]We combine our data with the literature CHARA K'-band data points, observed in 2006 with the S1/E1 baseline, published in Baines et al. (2008a) – see Section 4.4 for additional details.

Note. For details on the interferometric observations, see Section 2.1.

[1] This includes HD 107383 whose companion's minimum mass is around 20 Jupiter masses (Table 4) and could thus be considered a brown dwarf.

[2] As we show in Fig. 1 and Tables 1 and 2, our angular diameter fit for GJ 614 contains literature K' data obtained in 2006 and published in Baines et al. (2008a).

[3] Calibrated visibility data are available on request.

Table 2. Stellar angular diameters.

Star name	No. of Obs.	Reduced χ^2	$\theta_{UD} \pm \sigma$ (mas)	μ_λ	$\theta_{LD} \pm \sigma$ (mas)	θ_{LD} (per cent err)
61 Vir	16	0.31	1.037 ± 0.005	0.367	1.073 ± 0.005	0.4
ρ CrB	9	0.46	0.714 ± 0.013	0.342	0.735 ± 0.014	1.9
GJ 176	14	0.18	0.441 ± 0.020	0.210	0.448 ± 0.021	4.6
GJ 614	28[a]	1.16	0.449 ± 0.017	0.284	0.459 ± 0.017	3.7
GJ 649	18	1.02	0.472 ± 0.012	0.327	0.484 ± 0.012	2.5
GJ 876	33	0.32	0.721 ± 0.009	0.398	0.746 ± 0.009	1.2
HD 1461	16	0.19	0.483 ± 0.010	0.369	0.498 ± 0.011	2.1
HD 7924	15	0.19	0.424 ± 0.014	0.281	0.433 ± 0.014	3.2
HD 33564	16	1.08	0.629 ± 0.010	0.225	0.640 ± 0.010	1.6
HD 107383	7	0.16	1.590 ± 0.015	0.417	1.651 ± 0.016	1.0
HD 210702	16	1.57	0.845 ± 0.005	0.484	0.886 ± 0.006	0.6

[a]Includes CHARA classic K' data from Baines et al. (2008a).
Note. θ_{UD} and θ_{LD} refer to stellar uniform-disc and limb-darkening-corrected angular diameters, respectively. μ_λ are the limb-darkening coefficients from Claret (2000) after an iteration based on T_{eff} values. Refer to Section 2.1 for details.

and the wavelength of observation (Hanbury Brown et al. 1974).[4] The temperature-dependent limb-darkening coefficients, μ_λ, used to convert from θ_{UD} to θ_{LD}, are taken from Claret (2000) after we iterate based on the effective temperature value obtained from initial spectral energy distribution (SED) fitting (see Section 2.2). Limb-darkening coefficients are dependent on assumed stellar effective temperature, surface gravity, and weakly on metallicity. When we vary the input T_{eff} by 200 K and $\log g$ by 0.5 dex, the resulting variations are below 0.1 per cent in θ_{LD} and below 0.05 per cent in T_{eff}. Varying the assumed metallicity across the range of our target sample does not influence our final values of θ_{LD} and T_{eff} at all.

The values for θ_{UD} and θ_{LD} for our targets are given in Table 2. The angular diameters and their respective uncertainties are computed using MPFIT, a non-linear least-squares fitting routine in IDL (Markwardt 2009). Table 2 shows the empirical $\chi^2_{reduced}$ values of the fits shown in Figs 1 and 2 in column 3. These $\chi^2_{reduced}$ values are often calculated to be $\ll 1$ due to the difficulty of accurately defining uncertainties in the visibility measurements.[5] Consequently, we assume a true $\chi^2_{reduced} = 1$ when calculating the uncertainties for θ_{UD} and θ_{LD}, based on a rescaling of the associated uncertainties in the visibility data points. That is, the estimates of our uncertainties in θ_{UD} and θ_{LD} are based on a $\chi^2_{reduced}$ fit, not on strictly analytical calculations.

[4] Visibility is the normalized amplitude of the correlation of the light from two telescopes. It is a unitless number ranging from 0 to 1, where 0 implies no correlation, and 1 implies perfect correlation. An unresolved source would have perfect correlation of 1.0 independent of the distance between the telescopes (baseline). A resolved object will show a decrease in visibility with increasing baseline length. The shape of the visibility versus baseline is a function of the topology of the observed object (the Fourier Transform of the object's brightness distribution in the observed wavelength band). For a uniform disc this function is a Bessel function, and for this paper, we use a simple model of a limb darkened variation of a uniform disc.

[5] While there are methods of tracking errors through the calibration of visibility via standard statistical methods (e.g. van Belle & van Belle 2005), the principal difficulty in assessing a realistic estimate of the absolute error in visibility is the constantly changing nature of the atmosphere.

2.2 Bolometric fluxes

In this section, we report on stellar SED fits of our targets. We augment literature broad-band photometry data by using spectrophotometric data whenever available. The purpose of these SED fits is to obtain direct estimates of stellar T_{eff} and L, as described in Section 3.1. Our procedure is analogous to the ones performed in van Belle & von Braun (2009), von Braun et al. (2011a,b, 2012) and Boyajian et al. (2012a,b, 2013).

Our SED fitting is based on a χ^2-minimization of input SED templates from the Pickles (1998) to literature photometry of the star under investigation. If the literature photometry values are in magnitudes, they are converted to absolute fluxes by application of published or calculated zero-points. The filters of the literature photometry data are assumed to have a top-hat shape. That is, during the calculation of χ^2, only the central filter wavelengths are correlated with the SED template's flux value averaged over the filter transmission range in wavelength. Literature spectrophometry data are very useful for SED fitting since multiple individual photometry data points, instead of being integrated into a single wavelength, trace out the shape of the SED in great detail. The SED template is scaled to minimize χ^2 and then integrated over wavelength to obtain the bolometric flux. The code additionally produces an estimated angular diameter, which we only use as a sanity check to avoid systematic problems like the choice of wrong spectral template. Fig. 3 illustrates our procedure for the example of GJ 614.

We note that our quoted uncertainties on the bolometric flux values are statistical only. We do not (and indeed cannot) account for possible systematics such as saturation or correlated errors in the photometry, filter errors due to problems with transmission curves, or other non-random error sources. The only systematics that we can control are (1) the choice of spectral template for the SED fit, (2) the choice of which photometry data to include in the fit and (3) whether to let the interstellar reddening float during the fit or whether to set it to zero. In order to be consistent as possible, we take the following approach:

(i) All photometry data are included in the fit in principle, except when they present clear outliers in the SED. This way, we attempt to reduce systematics. In general, there are tens to hundreds of

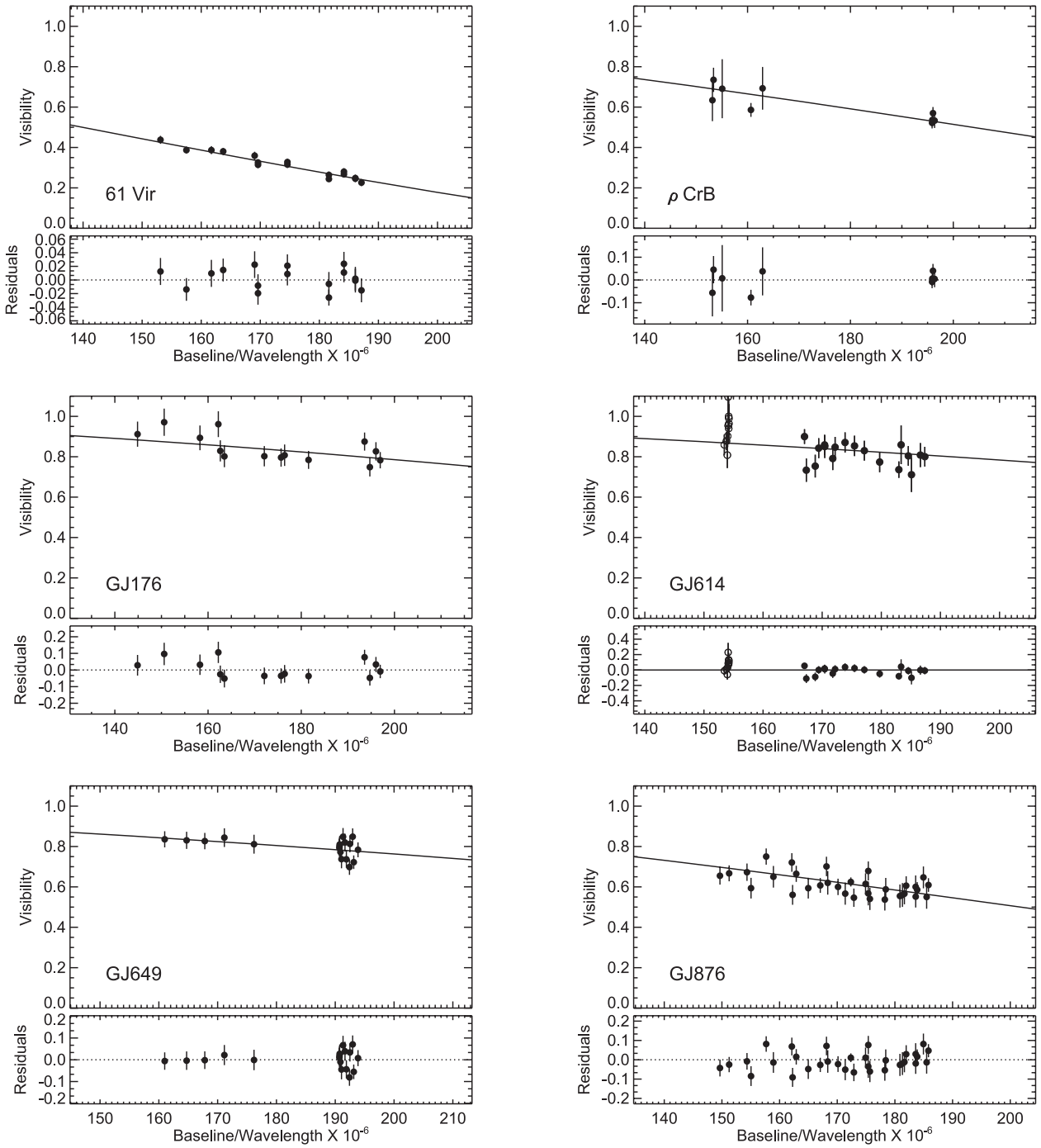

Figure 1. Plots of calibrated interferometric visibilities and fits. The separated cluster of data points shown as open circles in the visibility fit for GJ 614 with a relatively large spread in visibility that is located at smaller spatial frequencies (lower numeric values in baseline/wavelength) is comprised of literature K' data from Baines et al. (2008a) – see Section 4.4 for details. The interferometric observations are described in Section 2.1.

photometric measurements per target (see Table 3), and at most, we remove 1–2 data points, mostly in the *U* band or *RI* bands.

(ii) Interstellar extinction is set to zero for all targets, due to the small distances to the stars (see Table 4), which are adopted from van Leeuwen (2007). We cross-checked results with the ones using variable reddening, and in almost no case was there any difference. The ones for which the variable reddening produced results that are not consistent with $A_V = 0$ at the $\sim 1\sigma$ level are discussed below. For all others, letting A_V vary produced $A_V = 0$.

(iii) Whenever a literature photometry datum has no quoted uncertainty associated with it, we assign it a 5 per cent random uncertainty. This is only the case for some older data sets.

(iv) The choice of spectral template is based on minimization of $\chi^2_{\rm reduced}$ only. For about half of our targets, we linearly interpolate between the relatively coarse grid of the Pickles (1998) spectral templates to obtain a better fit and thus a more accurate value for the numerical integration to calculate the bolometric flux (indicated in Table 3). Linear interpolation never

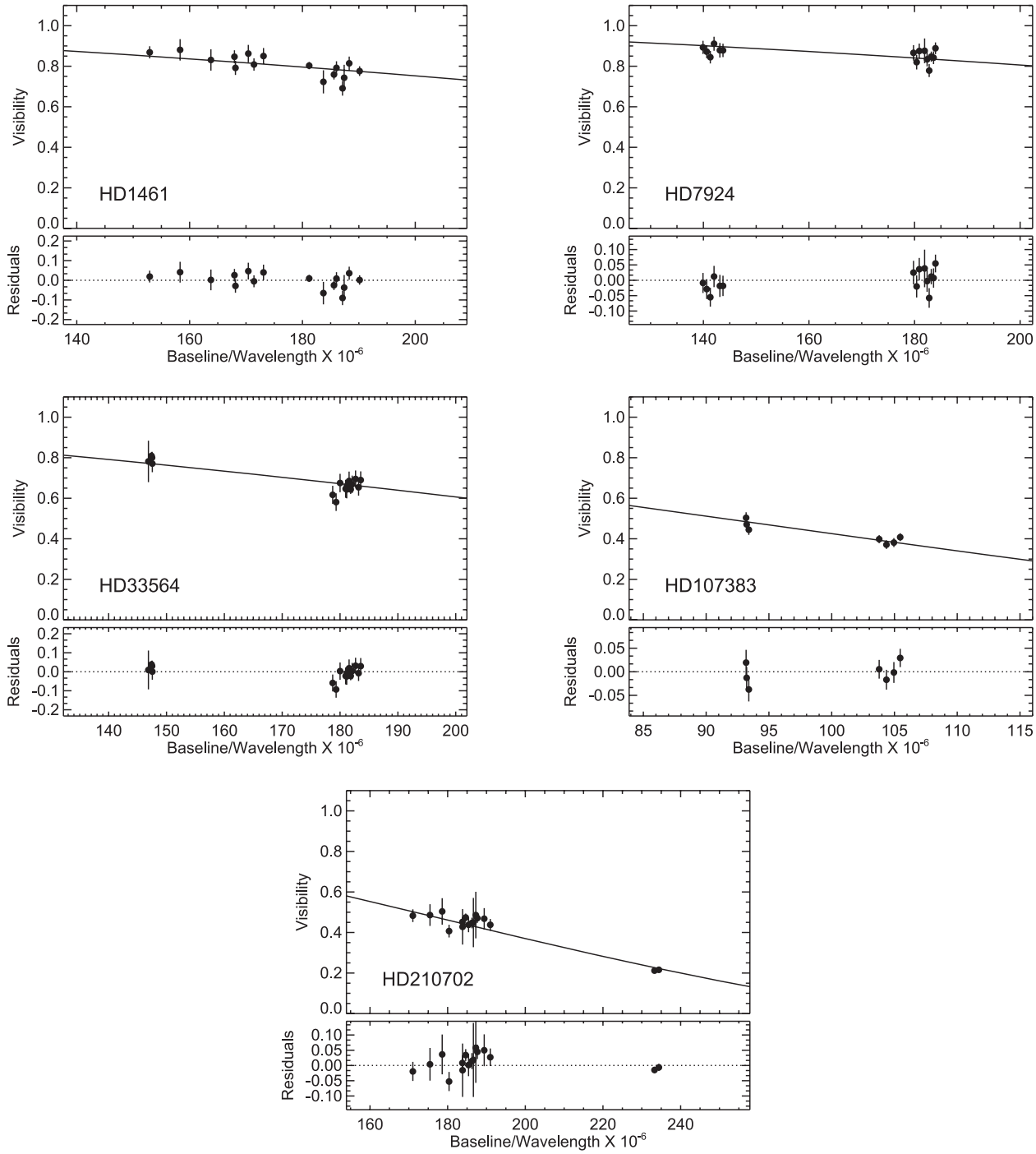

Figure 2. Plots of calibrated interferometric visibilities and fits. See Section 2.1 for details on the interferometric observations.

spans more than three tenths in spectral type range (e.g. G5 to G8).

(v) Despite the fact that spectrophotometry often increases the fit's $\chi^2_{\rm reduced}$, we include these data whenever available (indicated in Table 3) in order to reduce the systematics in the choice of spectral template, which is determined more accurately via spectrophotometry.

Notes on individual systems with respect to SED fitting.

(i) *61 Vir.* Despite the fact that we find $A_V = 0$ when letting A_V float, we note that dust excess for this system was reported in Trilling et al. (2008), Bryden et al. (2009), Lawler et al. (2009) and Tanner et al. (2009). Photometry sources: Johnson et al. (1966), Golay (1972), Johnson & Mitchell (1975), Dean (1981), Haggkvist & Oja (1987), Olsen (1994), Oja (1996); spectrophotometry from Burnashev (1985).

(ii) *ρ CrB.* Photometry sources: Argue (1963), Golay (1972), Clark & McClure (1979), Haggkvist & Oja (1987), Beichman et al. (1988), Jasevicius et al. (1990), Kornilov et al. (1991), Skiff (1994), Glushneva et al. (1998), Gezari, Pitts & Schmitz (1999), Cutri et al. (2003); spectrophotometry from Burnashev (1985).

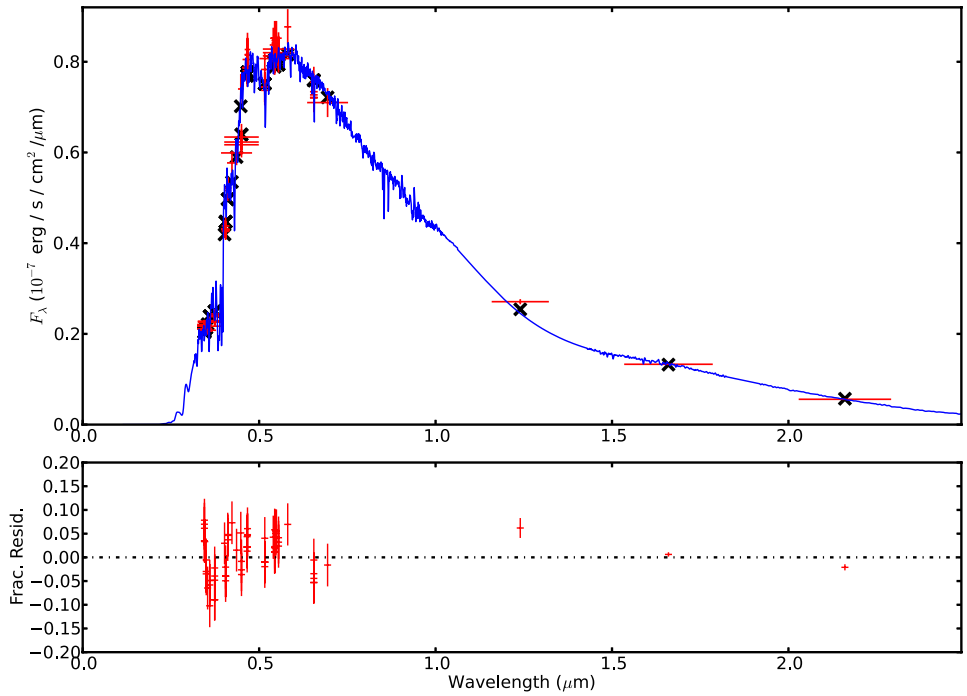

Figure 3. SED fit of GJ 614 to illustrate our fitting routine. In the top panel, the (blue) spectrum is a G9 IV spectral template from the Pickles (1998) library. The (red) crosses indicate photometry values from the literature. 'Error bars' in the x-direction represent the bandwidths of the photometric filters. The (black) X-shaped symbols indicate the flux value of the spectral template averaged over the filter transmission range in wavelength. The lower panel shows the residuals around the fit in fractional flux units of photometric uncertainty. The uncertainties in the y-direction in the lower plot represent the photometric uncertainties in the literature data scaled by the corresponding flux values. For more details, see Section 2.2.

Table 3. $F_{\rm BOL}$ values from SED fitting.

star	Template sp. type	Degrees of Freedom	$\chi^2_{\rm red}$	$F_{\rm BOL} \pm \sigma$ (10^{-8} erg s^{-1} cm^{-2})
61 Vir	G6.5V[a]	233[b]	2.81	36.06 ± 0.05
ρ CrB	G0V	369[b]	8.74	18.03 ± 0.02
GJ 176	M2.5V	36	5.95	1.26 ± 0.005
GJ 614	G9IV[a]	69	1.28	6.50 ± 0.02
GJ 649	M2V	32	8.90	1.30 ± 0.005
GJ 876	M3.5V[a]	109	7.18	1.78 ± 0.004
HD 1461	G2IV	91	0.63	6.95 ± 0.03
HD 7924	K0.5V[a]	16	2.37	4.14 ± 0.03
HD 33564	F6V	119[b]	4.88	23.17 ± 0.04
HD 107383	K0.5III[a]	68	1.60	44.49 ± 0.25
HD 210702	G9III[a]	47	0.79	13.65 ± 0.09

Note. For more details, please see Section 2.2.
[a]Linearly interpolated between Pickles (1998) spectral templates.
[b]Includes spectrophotometry.

(iii) *GJ 176*. Photometry sources: Weis (1984), Stauffer & Hartmann (1986), Weis (1986), Weis (1987), Weis (1993), Weis (1996), Gezari et al. (1999), Bessell (2000), Cutri et al. (2003).

(iv) *GJ 614*. Photometry sources: Argue (1963), Golay (1972), Beichman et al. (1988), Kornilov et al. (1991), Cutri et al. (2003), Kazlauskas et al. (2005).

(v) *GJ 649*. Photometry sources: Mumford (1956), Jones, Sinclair & Alexander (1981), Mermilliod (1986), Stauffer & Hartmann (1986), Beichman et al. (1988), Weis (1993), Weis (1996), Cutri et al. (2003), Kazlauskas et al. (2005).

(vi) *GJ 876*. With a variable A_V, the SED fit for GJ 876 produces slightly different results compared to the ones given in Table 3, where it was set to zero: $\chi^2_{\rm red} = 4.86$, $F_{\rm BOL} = (1.95 \pm 0.001) \times 10^{-8}$ erg s^{-1} cm^{-2} with an $A_V = 0.111 \pm 0.007$. Photometry sources: Erro (1971), Iriarte (1971), Golay (1972), Mould & Hyland (1976), Persson, Aaronson & Frogel (1977), Jones et al. (1981), Weis & Upgren (1982), The, Steenman & Alcaino (1984), Kozok (1985), Weis (1986), Weis (1987), Bessel (1990), Weis (1996), Bessell (2000), Koen et al. (2002), Cutri et al. (2003), Kilkenny et al. (2007), Koen et al. (2010).

(vii) *HD 1461*. Photometry sources: Cousins & Stoy (1962), Golay (1972), Sperauskas, Bartkevicius & Zdanavicius (1981), Haggkvist & Oja (1987), Kornilov et al. (1991), Cutri et al. (2003), Kazlauskas et al. (2005).

(viii) *HD 7924*. Photometry sources: Sanders (1966), Golay (1972), Kornilov et al. (1991), Cutri et al. (2003).

(ix) *HD 33564*. With a variable A_V, the SED fit for HD 33564 produces slightly different results compared to the ones given in Table 3: $\chi^2_{\rm red} = 3.81$, $F_{\rm BOL} = (25.05 \pm 0.19) \times 10^{-8}$ erg s^{-1} cm^{-2} with an $A_V = 0.076 \pm 0.007$. Photometry sources: Häggkvist & Oja (1966), Golay (1972), Beichman et al. (1988), Cernis et al. (1989), Gezari et al. (1999), Kornilov et al. (1991), Cutri et al. (2003); spectrophotometry from Kharitonov, Tereshchenko & Knjazeva (1988).

(x) *HD 107383*. Photometry sources: Johnson et al. (1966), Häggkvist & Oja (1970), Straizys (1970), Golay (1972), Johnson & Mitchell (1975), Beichman et al. (1988), Kornilov et al. (1991), Yoss & Griffin (1997), Cutri et al. (2003).

(xi) *HD 210702*. With a variable A_V, the SED fit for HD 210702 produces marginally different results compared to the ones given in Table 3: $\chi^2_{\rm red} = 0.77$, $F_{\rm BOL} = (14.24 \pm 0.05) \times 10^{-8}$ erg s^{-1} cm^{-2} with an $A_V = 0.037 \pm 0.029$. Photometry sources: Johnson & Knuckles (1957), Johnson et al. (1966), Golay (1972), Olson

Table 4. Stellar astrophysical parameters.

Star	Radius ($R_\odot$)	$T_{\rm eff}$ (K)	L ($L_\odot$)	Spectral type	Distance (pc)	Metallicity [Fe/H]	$HZ_{\rm cons}$ (au)	$HZ_{\rm opt}$ (au)	Age (Gyr)	Mass ($M_\odot$)
61 Vir	0.9867 ± 0.0048	5538 ± 13	0.8222 ± 0.0033	G7 V	8.56	0.01	0.91–1.56	0.69–1.63	8.6	0.93
ρ CrB	1.3617 ± 0.0262	5627 ± 54	1.7059 ± 0.0423	G0 V	17.43	− 0.22	1.30–2.23	0.98–2.33	12.9	0.91
GJ 176	0.4525 ± 0.0221	3679 ± 77	0.0337 ± 0.0018	M2	9.27	0.15[a]	0.20–0.37	0.15–0.38	–	0.45[b]
GJ 614	0.8668 ± 0.0324	5518 ± 102	0.6256 ± 0.0077	K0 IV–V	15.57	0.44	0.79–1.37	0.60–1.43	–	0.91[b]
GJ 649	0.5387 ± 0.0157	3590 ± 45	0.0432 ± 0.0013	M0.5	10.34	− 0.04[a]	0.22–0.42	0.17–0.44	–	0.54[b]
GJ 876	0.3761 ± 0.0059	3129 ± 19	0.0122 ± 0.0002	M4	4.69	0.19[a]	0.12–0.23	0.09–0.24	–	0.37[b]
HD 1461	1.2441 ± 0.0305	5386 ± 60	1.1893 ± 0.0476	G3 V	23.44	0.16	1.10–1.89	0.83–1.98	13.8	0.94
HD 7924	0.7821 ± 0.0258	5075 ± 83	0.3648 ± 0.0077	K0 V	16.82	− 0.14	0.62–1.08	0.47–1.13	–	0.81[b]
HD 33564	1.4367 ± 0.0238	6420 ± 50	3.1777 ± 0.0696	F7 V	20.98	0.08	1.73–2.88	1.31–3.00	2.2	1.31
HD 107383	15.781 ± 0.3444	4705 ± 24	109.51 ± 4.3256	K0 III	88.89	− 0.30	10.8–19.4	8.19–20.3	–[c]	–[c]
HD 210702	5.2314 ± 0.1171	4780 ± 18	12.838 ± 0.5569	K1 III	54.95	0.03[d]	3.70–6.59	2.80–6.90	5.0	1.29

Note. For the calculations of stellar R, $T_{\rm eff}$ and L, please see Section 3.1. Spectral types and metallicities from Anderson & Francis (2011, 2012) unless otherwise indicated. Distances from van Leeuwen (2007). The calculations for the inner and outer boundaries of the system circumstellar HZs (conservative and optimistic) and for stellar mass and age are described in Section 3.2.

[a]From Rojas-Ayala et al. (2012). Each value has a quoted uncertainty of 0.17 dex.

[b]Masses calculated via equation (2), based on data in Boyajian et al. (2012b).

[c]Beyond the range of the Y^2 isochrones.

[d]From Maldonado, Villaver & Eiroa (2013).

(1974), McClure & Forrester (1981), Kornilov et al. (1991), Cutri et al. (2003).

3 STELLAR ASTROPHYSICAL PARAMETERS

In this section, we report on our direct measurements of stellar diameters, $T_{\rm eff}$, and luminosities, based on our interferometric measurements (Section 2.1) and SED fitting to literature photometry (Section 2.2). We furthermore present calculated values wherever sensible for our targets, such as the location and extent of the respective system's circumstellar HZ and stellar mass and age. Results are summarized in Table 4.

3.1 Direct: stellar radii, effective temperatures and luminosities

We use our measured, limb-darkening corrected, angular diameters $\theta_{\rm LD}$, corresponding to the angular diameter of the Rosseland, or mean, radiating surface of the star (Section 2.1, Table 2), coupled with trigonometric parallax values from van Leeuwen (2007) to determine the linear stellar diameters. Uncertainties in the physical stellar radii are typically dominated by the uncertainties in the angular diameters, not the distance.

From the SED fitting (Section 2.2, Table 3), we calculate the value of the stellar bolometric flux, $F_{\rm BOL}$ by numerically integration of the scaled spectral template across all wavelengths. Wherever the empirical spectral template does not contain any data, it is interpolated and extrapolated along a blackbody curve. Combination with the rewritten version of the Stefan–Boltzmann Law

$$T_{\rm eff}({\rm K}) = 2341 \left(F_{\rm BOL}/\theta_{\rm LD}^2\right)^{1/4}, \quad (1)$$

where $F_{\rm BOL}$ is in units of 10^{-8} erg cm^{-2} s^{-1} and $\theta_{\rm LD}$ is in units of mas, produces the effective stellar temperatures $T_{\rm eff}$.

3.2 Calculated: HZs, stellar masses and ages

To first order, the HZ of a planetary system is described as the range of distances in which a planet with a surface and an atmosphere containing a modest amount of greenhouse gases would be able to host liquid water on its surface, first characterized in Kasting, Whitmire & Reynolds (1993). The HZ boundaries in this paper are calculated based on the updated formalism of Kopparapu et al. (2013a,b).[6] Kopparapu et al. (2013a) define the boundaries based on a runaway greenhouse effect or a runaway snowball effect as a function of stellar luminosity and effective temperature, plus water absorption by the planetary atmosphere. Whichever assumption is made of how long Venus and Mars were able to retain liquid water on their respective surfaces defines the choice of HZ (conservative or optimistic). These conditions are described in more detail in Kopparapu et al. (2013a) and section 3 of Kane, Barclay & Gelino (2013). The boundaries quoted in Table 4 are the ones for both the conservative and optimistic HZ.

For stellar mass and age estimates of the early stars in our sample, we use the Yonsei–Yale (Y^2) isochrones (Yi et al. 2001; Kim et al. 2002; Demarque et al. 2004). Input data are our directly determined stellar radii and temperatures, along with the literature metallicity values from Table 4, and zero α-element enhancement: [α/Fe] = 0. We follow the arguments in section 2.4 in Boyajian et al. (2013) and conservatively estimate mass and age uncertainties of 5 per cent and 5 Gyr, respectively.

The ages of low-mass stars, however, are not sensitive to model isochrone fitting. Thus, in order to estimate the stellar masses of the KM dwarfs in our sample, we use the formalism described in section 5.4 in Boyajian et al. (2012b). We use the data from table 6 in Boyajian et al. (2012b) to derive the following equation for KM dwarfs:

$$M = -0.0460(\pm 0.0251) + 1.0930(\pm 0.1481)R + 0.0064(\pm 0.1722)R^2, \quad (2)$$

where R and M are the stellar radius and mass in Solar units, respectively. This essentially represents the inverted form of equation 10 in Boyajian et al. (2012b) for single dwarf stars. We note that the statistical errors in the determined masses using equation (2) are dominated by the uncertainties in the coefficients and are of the order of ∼30 per cent.

[6] We use the online calculator at http://www3.geosc.psu.edu/~ruk15/planets/

4 DISCUSSION

In this section, we briefly discuss our results on the individual systems. We compare our directly determined stellar parameters (Section 3.1 and Table 4) to quoted literature values. Statistical differences between values are calculated by adding our uncertainties and those from the literature, when available, in quadrature.

4.1 61 Vir (= HD 115617)

61 Vir hosts three planets with periods ranging from 4.2 to 124 d and minimum masses between 5.1 and 24 $M_\oplus$ (Vogt et al. 2010). Since the orbital distances of all three planets are less than 0.5 au from the parent star, and since the inner edge of the optimistic/conservative HZ is located at 0.69 au/0.91 au, none of the known three planets reside within the system's HZ.

The stellar radius for 61 Vir quoted in Takeda et al. (2007, $0.98 \pm 0.03\,R_\odot$) is statistically identical with ours. When compared to Valenti & Fischer (2005), our radius measurement is $\sim 2\sigma$ larger than their estimate ($0.963 \pm 0.011\,R_\odot$), while our temperature value is consistent with their value (5571 ± 44 K). Similarly good agreement exists with the $T_{\rm eff}$ value quoted in Ecuvillon et al. (2006, 5577 ± 33 K).

To estimate 61 Vir's mass and age, we use the Y^2 isochrones with our values from Table 4 as input, generated with a 0.1 Gyr step size, and a fixed metallicity of [Fe/H] = +0.01 (Table 4). Interpolation within the best-fitting isochrone gives an age of 8.6 Gyr and mass of $0.93\,M_\odot$.

4.2 ρ CrB (= HD 143761)

ρ CrB has a Jupiter-mass planet in a 40 d orbit (Noyes et al. 1997) whose orbital semimajor axis (0.22 au; Butler et al. 2006) is located well inside the system's optimistic/conservative HZ's inner boundary at 0.98 au/1.3 au.

ρ CrB's radius was interferometrically observed in the K' band by Baines et al. (2008a) who calculated a radius of $1.284 \pm 0.082\,R_\odot$, well within 1σ of our value of $1.3424\,R_\odot$. ρ CrB's stellar radius from Fuhrmann, Pfeiffer & Bernkopf (1998), $1.34 \pm 0.05\,R_\odot$, also agrees very well ($\ll 1\sigma$) with our directly determined value. The spectroscopically determined $T_{\rm eff}$ values of Fuhrmann et al. (1998, 5821 ± 80 K) and Valenti & Fischer (2005, 5822 ± 44 K), however, come in at 1.8σ and 2.7σ above our estimate of 5665 K.

Using the same procedure as for 61 Vir (Section 4.1), we solve for best-fitting Y^2 isochrone properties for ρ CrB using a metallicity of [Fe/H] = −0.22 (Table 4). This produces estimates for stellar age of 12.9 Gyr and stellar mass of $0.91\,M_\odot$.

4.3 GJ 176 (= HD 285968)

The 8.8 Earth-mass planet in a 10.24 d, circular orbit around GJ 176 (Endl et al. 2008; Forveille et al. 2009) is at a projected semimajor axis of less than 0.07 au from its parent star, well inside the inner boundary of the system optimistic/conservative HZ at 0.15 au/0.2 au.

Takeda (2007) estimate GJ 176's stellar radius to be $0.46^{+0.01}_{-0.02}\,R_\odot$, statistically identical to our directly determined value of $0.4525\,R_\odot$. The $T_{\rm eff}$ estimate in Morales, Ribas & Jordi (2008, 3520 K) is around 2σ below our value, in part due to the fact, however, that no uncertainties in $T_{\rm eff}$ are provided. Finally, our values are in agreement with $T_{\rm eff} = 3754$ K and $R = 0.40\,R_\odot$ from Wright et al. (2011b).

We estimate the mass of GJ 176 to be $0.45\,M_\odot$ via equation (2). It is possible, but extremely unreliable, to estimate isochronal ages for low-mass stars, as stated earlier in Section 3.2.

4.4 GJ 614 (= HD 145675 = 14 Her)

The planet in orbit around GJ 614 was first announced by M. Mayor in 1998 (see http://obswww.unige.ch/∼udry/planet/14her.html). Butler et al. (2003) provide system characterization, including the period of around 4.7 yr with an eccentricity of 0.37 and a planet minimum mass of about 4.9 Jupiter masses. At a projected semimajor axis of 2.82 au, this planet is actually located outside the system optimistic/conservative HZ's outer edge at 1.43 au/1.37 au, even at periastron distance $r_{\rm peri} = (1 - e)a = 1.78$ au.

Baines et al. (2008a) interferometrically determine GJ 614's physical radius to be $0.708 \pm 0.85\,R_\odot$, which is around 1.9σ below our value. Those data are taken in the K' band, where GJ 614's small angular diameter is only marginally resolved. Since the Baines et al. (2008a) K' band data alone thus do not constrain the angular diameter fit as well as our H data, we combine the Baines et al. (2008a) visibilities along with our own to determine GJ 614's angular diameter in Table 2 and linear radius in Table 4. Our H-band data enable increased resolution due to the shorter wavelengths (see Fig. 1, where the Baines et al. 2008a calibrated visibilities are represented by the cluster of data points with relatively large scatter at shorter effective baseline values).

There are a large number (many tens on Vizier) of $T_{\rm eff}$ values in the literature with estimates between 4965 and 5735 K, which average slightly over 5300 K. The catalogue in Soubiran et al. (2010) alone contains 19 values between 5129 K (Ramírez & Meléndez 2005) and 5600 K (Heiter & Luck 2003). Our value of 5518 ± 102 K falls towards the upper tier of the literature range.

Using equation (2), we derive the stellar mass for GJ 614 to be $0.91\,M_\odot$.

4.5 GJ 649

GJ 649 hosts a 0.33 $M_{\rm Jup}$ planet in an eccentric 598.3 d orbit with a semimajor axis of 1.135 au (Johnson et al. 2010). We calculate GJ 649's circumstellar optimistic/conservative HZ's outer boundary to be 0.44 au/0.42 au, putting the planet well beyond the outer edge of the system HZ, even at periastron.

Our estimate for GJ 649's radius is $0.5387 \pm 0.0157\,R_\odot$, which falls in the middle between the values in Takeda (2007, $0.46^{+0.01}_{-0.02}\,R_\odot$), Zakhozhaj (1979, $0.49\,R_\odot$) and Houdebine (2010, $0.616 \pm 0.026\,R_\odot$).

Our effective temperature for GJ 649 is 3590 ± 45 K, which also falls in the middle of a fairly large range in the literature values: Lafrasse et al. (2010a, 3370 K), Ammons et al. (2006, 4185^{+161}_{-334} K), Soubiran et al. (2010, 3717, 3782 ± 58 K), Morales et al. (2008, 3670 K) and Houdebine (2010, 3503 ± 50 K).

Applying equation (2) to our radius value produces a mass value for GJ 649 of $0.54\,M_\odot$.

4.6 GJ 876

The late-type, multiplanet host GJ 876 has been studied extensively. There are four planets in orbit around the star (Correia et al. 2010; Rivera et al. 2010b) at an inclination angle with respect to the plane of the system of 59°.5. The planet masses range from 6.83 $M_\oplus$ to $2.28 M_{\rm Jup}$ in orbital distances that range from 0.02 to 0.33 au with periods between 1.94 and 124.26 d (Rivera et al. 2010b). Based on

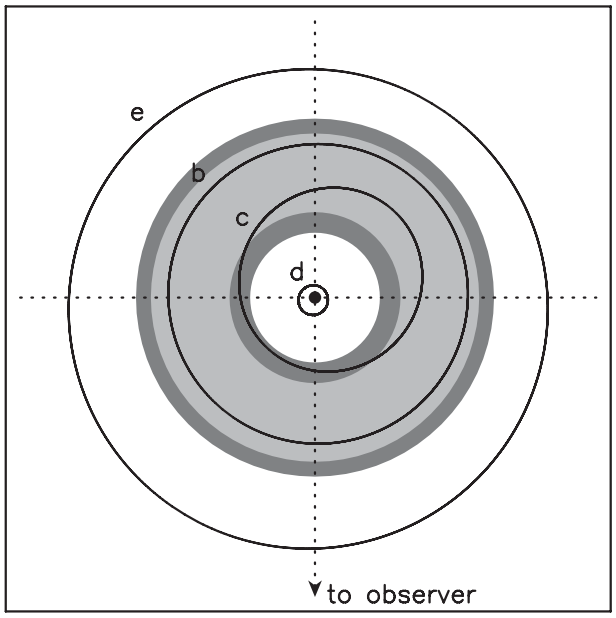

Figure 4. Architecture of the GJ 876 system. The conservative HZ is shown in light grey, the optimistic HZ comprises both the light grey and dark grey regions. Planets b and c spend their entire orbits in the optimistic HZ. Planet b spends its entire orbit in the conservative HZ, whereas planet c spends 68.5 per cent of its orbital period in it. For details, see Section 3, Section 4.6 and Table 4. Orbital parameters for the planets are taken from Rivera et al. (2010b). For scale: the size of the box is 0.8 au × 0.8 au.

our optimistic/conservative HZ boundaries of 0.09–0.24 au/0.12–0.23 au in Table 4, two of the planets (b and c) are located within the system HZ. For an image of the system architecture, see Fig. 4.

We use the methods outlined in section 4 and equation 2 in von Braun et al. (2011b), based on the work of Selsis et al. (2007), to calculate the equilibrium temperatures $T_{\rm eq}$ for the GJ 876 planets via the equation

$$T_{\rm eq}^4 = \frac{S(1-A)}{f\sigma}, \quad (3)$$

where S is the stellar energy flux received by the planet, A is the Bond albedo and σ is the Stefan–Boltzmann constant (Selsis et al. 2007).

We differentiate between two scenarios, which are dependent on the efficiency of the heat distribution across the planet by means of winds, circulation patterns, streams, etc. The energy redistribution factor f is set to 2 and 4 for low- and high-energy redistribution efficiency, respectively. Assuming a Bond albedo value of 0.3 the planetary equilibrium temperatures for $f = 4$ are 587 K (planet d), 235 K (planet c), 186 K (planet b) and 147 K (planet e). The $T_{\rm eq}$ values for $f = 2$ are 698 K (d), 280 K (c), 221 K (b) and 174 K (e). These values scale as $(1 - A)^{1/4}$ for other Bond albedo values (equation 3).

Previously estimated values for GJ 876's stellar radius are significantly below our directly determined value of $0.3761 \pm 0.0059\,{\rm R}_\odot$: $0.24\,{\rm R}_\odot$ (Zakhozhaj 1979) and $0.3\,{\rm R}_\odot$ (Laughlin et al. 2005; Rivera et al. 2010b), the latter of which is the one that is frequently used in the exoplanet literature about GJ 876. In comparison to our value of $T_{\rm eff} = 3129 \pm 19$ K, the literature temperatures for GJ 876 include a seemingly bimodal distribution of values: 3130 K (Dodson-Robinson et al. 2011), 3165 ± 50 K (Houdebine 2012), 3172 K (Jenkins et al. 2009), 3765^{+477}_{-650} K (Ammons et al. 2006) and 3787 K (Butler et al. 2006).

Finally, we derive a mass for GJ 876 of $M = 0.37\,{\rm M}_\odot$ using equation (2).

4.7 HD 1461

HD 1461 hosts two super-Earths in close proximity to both the star and each other: a 7.6 Earth-mass planet in a 5.8 d orbit (Rivera et al. 2010a) and a 5.9 Earth-mass planet in a 13.5 d orbit (Mayor et al. 2011, both are minimum masses). Their semimajor axes are 0.063 and 0.112 au, respectively, all well inside HD 1461's HZ, whose inner optimistic/conservative boundary is at 0.83 au/1.10 au.

Our radius estimate of $1.1987 \pm 0.0275\,{\rm R}_\odot$ is larger at the $>2\sigma$ level than both radius estimates in the literature: $1.11 \pm 0.04\,{\rm R}_\odot$ (Takeda 2007) and $1.0950 \pm 0.0260\,{\rm R}_\odot$ (Valenti & Fischer 2005).

We measure an effective temperature for HD 1461 to be 5486 ± 52 K, which falls below all of the many temperature estimates in the literature for HD 1461 – a sensible consequence given that our radius is larger than literature estimates. The Soubiran et al. (2010) catalogue alone has 13 different $T_{\rm eff}$ values, ranging from 5683 to 5929 K. Additionally, we find temperature estimates of 5688 K (Holmberg, Nordström & Andersen 2009), 5666 ± 42 K (Prugniel, Vauglin & Koleva 2011) and 5588 ± 64 K (Koleva & Vazdekis 2012).

We use the Y^2 isochrones following the method described in Section 3.2 to derive and age and mass of HD 1461. We obtain a mass of $0.94\,{\rm M}_\odot$ and an age of 13.8 Gyr.

4.8 HD 7924

The super-Earth ($M \sin i = 9.26\,{\rm M}_\oplus$) orbits HD 7924 at a period of 5.4 d and at a semimajor axis of 0.057 au (Howard et al. 2009). The inner boundary of the optimistic/conservative HD 7924 system is at 0.47 au/0.62 au from the star, well beyond the planetary orbit.

The radius of HD 7924 has been estimated to be $R = 0.78 \pm 0.02\,{\rm R}_\odot$ (Takeda 2007), which is identical to our direct measurement of $R = 0.7821\,{\rm R}_\odot$. The radius estimate of $R = 0.754\,{\rm R}_\odot$ (Valenti & Fischer 2005) is slightly below but consistent with our value.

Our effective temperature measurement $T_{\rm eff} = 5075$ K falls into the middle of a large effective temperature range present in the literature for HD 7924: 4550 K (Lafrasse et al. 2010a), 4750 K (Wright et al. 2003), 5111^{+113}_{-128} K (Ammons et al. 2006), 5121–5177 K (six entries; Soubiran et al. 2010), 5177 K (Petigura & Marcy 2011), 5177 K (Valenti & Fischer 2005), 5153 ± 5.8 K (Kovtyukh, Soubiran & Belik 2004) and 5165 K (Mishenina et al. 2008, 2012).

Our derived mass from equation (2) is $M = 0.81\,{\rm M}_\odot$.

4.9 HD 33564

HD 33564 hosts a $M \sin i = 9.1 M_{\rm Jup}$ planet in an eccentric 388 d orbit (Galland et al. 2005) and an orbital semimajor axis of 1.1 au. Since the orbital eccentricity is 0.34, its apastron distance is $r_{\rm ap} = (1 + e)a = 1.47$ au. While the conservative HZ is located beyond HD 33564b's orbit, the planet spends around 43 per cent of its orbital duration inside the optimistic HZ, whose inner edge is at 1.31 au. HD 33564's system architecture is shown in Fig. 5.

We measure HD 33564's radius to be $1.4712 \pm 0.0219\,{\rm R}_\odot$. This is consistent with the previous estimate based on SED fitting by van Belle & von Braun (2009) of $R = 1.45 \pm 0.03\,{\rm R}_\odot$.

Our value for the effective temperature of HD 33564 is 6346 ± 44 K, which is largely consistent with the considerable number of estimates available in the literature: $T_{\rm eff} = 6440$ K (Wright

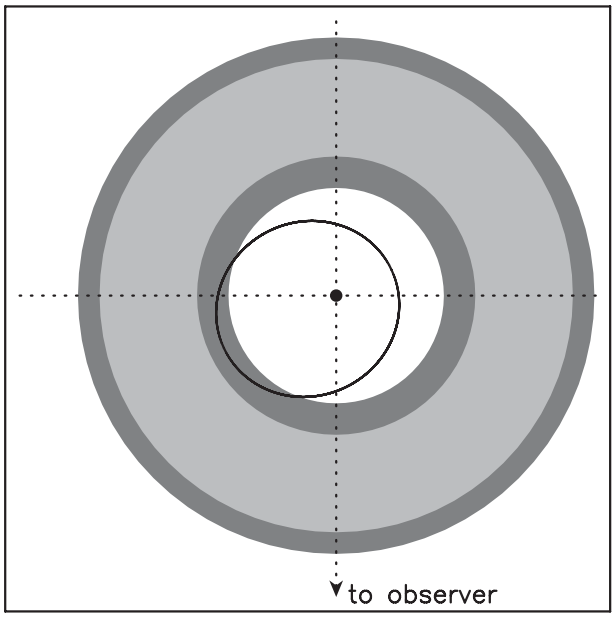

Figure 5. Architecture of the HD 33564 system. The conservative HZ is shown in light grey, the optimistic HZ comprises both the light grey and dark grey regions. The planet in orbit around HD 33564 spends ∼43 per cent of its orbital period in the optimistic HZ. For details, see Section 3, Section 4.9 and Table 4. Orbital parameters are from Galland et al. (2005). The size of the box is 7 au × 7 au.

et al. 2003), 6302 K (Marsakov & Shevelev 1995), 6597^{+17}_{-708} K (Ammons et al. 2006), 6307–6554 K (three entries; Soubiran et al. 2010), 6250 ± 150 K (Butler et al. 2006), 6531 ± 70 K (van Belle & von Braun 2009), 6456 K (Allende Prieto & Lambert 1999), 6233 K (Schröder, Reiners & Schmitt 2009), 6379 ± 80 K (Casagrande et al. 2011), 6307 K (Eiroa et al. 2013), 6394 K (Gray et al. 2003), 6250 K (Dodson-Robinson et al. 2011) and 6554 ± 93 K (Gonzalez, Carlson & Tobin 2010).

We estimate a mass of HD 33564 to be 1.31 $M_\odot$ at an isochronal age of 2.2 Gyr.

4.10 HD 107383 (= 11 Com)

The giant star HD 107383 has a substellar-mass companion in an eccentric 328 d orbit at a semimajor axis of 1.29 au (Liu et al. 2008). Since HD 107383's luminosity is more than 100 times that of the sun, however, its optimistic/conservative HZ's inner boundary is at 8.19 au/10.83 au, well beyond even the apastron of the known companion.

Our radius estimate for the giant star HD 107383 is 15.78 ± 0.34 $R_\odot$ – no previous radius estimates appear in the literature for this star. We measure an effective temperature for HD 107383 to be 4705 ± 24 K, which falls into the middle of previously published values: 4900 K (Wright et al. 2003), 4717^{+381}_{-283} K (Ammons et al. 2006), 4690 K (McWilliam 1990), 4880 K (Hekker & Meléndez 2007), 4690 K, (Valdes et al. 2004), 4804 K (Schiavon 2007), 4806 ± 34 K (Wu et al. 2011), 4690 K (Manteiga et al. 2009) and 4873 K (Luck & Heiter 2007).

The evolutionary status and consequently the luminosity of this K0 giant are located outside of the range of the Y^2 isochrones. In addition, the star is evolved, and thus, equation (2) is not applicable. We therefore cannot calculate its age or mass.

4.11 HD 210702

HD 210702 hosts a $M \sin i = 1.9 M_{\rm Jup}$ planet in a low-eccentricity, 355 d orbit (Johnson et al. 2007). With a semimajor axis of 1.2 au, the planet does not enter the system conservative or optimistic HZs, even at apastron.

We measure HD 210702's radius and $T_{\rm eff}$ to be 5.2314 ± 0.1171 $R_\odot$ and 4780 ± 18 K, respectively, which is consistent with the interferometric (CHARA K'-band) values published in Baines et al. (2009, 5.17 ± 0.15 $R_\odot$ and 4859 ± 62 K), as well as the radius estimated in the XO-Rad catalogue of van Belle & von Braun (2009, 5.20 ± 0.31 $R_\odot$). Allende Prieto & Lambert (1999) quote 5.13 $R_\odot$ and 4897 K (with error estimates for all stars in their catalogue of 6 per cent in radius and 2 per cent in $T_{\rm eff}$) – also consistent with our direct values. Other estimates from Johnson et al. (2007, 4.45 ± 0.07 $R_\odot$ and 5510 ± 44 K) and Maldonado et al. (2013, 4.7 $R_\odot$ and 4993 K) are lower in radius and higher in effective temperature than our directly determined values.

Application of the Y^2 isochrones with input values from Table 4 for HD 210702 returns a stellar age of 5 Gyr and a mass of 1.29 $M_\odot$.

5 SUMMARY AND CONCLUSION

A very large fraction of the information on extrasolar planets that has been gathered over the course of the last 20 yr is purely due to the study of the effects that the planets have on their respective parent stars. That is, the star's light is used to characterize the planetary system. In addition, the parent star dominates any exoplanet system as the principal energy source and mass repository. Finally, physical parameters of planets are almost always direct functions of their stellar counterparts. These aspects assign a substantial importance to studying the stars themselves: one at best only understands the planet as well as one understands the parent star.

In this paper, we characterize 11 exoplanet host star systems with a wide range in radius and effective temperature, based on a 3.5 yr long observing survey with CHARA's Classic beam combiner. For the systems with previously published direct diameters (ρ CrB, GJ 614 and HD 210702), we provide updates based on increased data quantity and improved performance by the array. For the rest of the systems, only indirectly determined values for radius and effective temperature are present in the literature (if any exist at all). Our thus determined stellar astrophysical parameters make it possible to place our sample of exoplanet host stars on to an empirical Hertzsprung–Russell (H–R) diagram. In Fig. 6, we show our targets along with interferometrically determined parameters of previously published exoplanet hosts and other main-sequence stars with diameter uncertainties of less than 5 per cent.

Due to the relatively low number of stars per spectral type in our sample, and due to the large variance among radius and temperature values quoted in the literature, it is impossible to quantify trends in terms of how indirectly determined values compare with direct counterparts as a function of spectral type, such as the ones documented in Boyajian et al. (2013). For the latest spectral type in our sample, and arguably the most interesting system in terms of exoplanet science, GJ 876, our directly determined stellar radius is significantly (>20 per cent) larger than commonly used literature equivalents (Section 4.6).

We use our directly determined stellar properties to calculate stellar mass and age wherever possible, though the associated uncertainties are large for the KM dwarfs (Section 3.2). Calculations of system HZ locations and boundaries, based on stellar luminosity and effective temperature, show that (1) GJ 876 hosts two planets

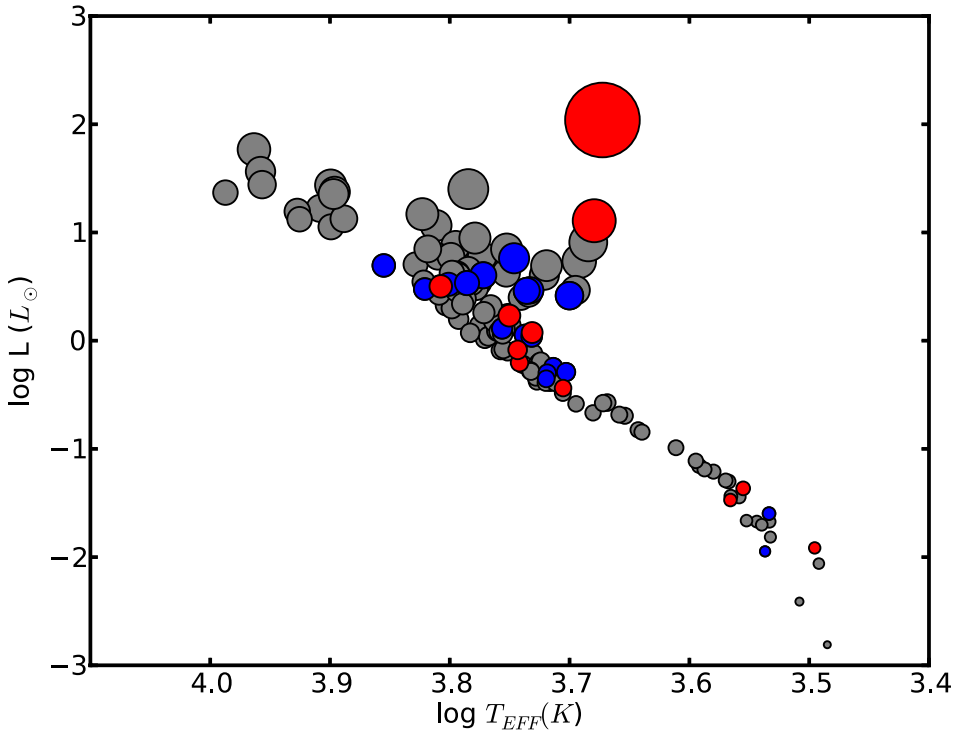

Figure 6. Empirical H–R diagram for all main-sequence stars with interferometrically determined radii whose random uncertainties are smaller than 5 per cent, as published and compiled in Boyajian et al. (2012b, 2013). The diameter of each data point is representative of the respective stellar radius. Error bars in effective temperature and luminosity are smaller than the size of the data points. Previously published exoplanet host stars are identified in blue (Kervella et al. 2003; Baines et al. 2008a, 2009; van Belle & von Braun 2009; von Braun et al. 2011a,b, 2012; Boyajian et al. 2013; Henry et al. 2013). The exoplanet host stars that are presented in this work are shown in red. Stars that do not host any published exoplanets are shown in grey.

who spend all or large parts of their orbital duration in the system HZ, whereas (2) the planet orbiting HD 33564 spends a small part of its period in the stellar HZ as its elliptical orbit causes it to periodically dip into it around apastron passage.

CHARA's continuously improving performance in both sensitivity and spatial resolution increasingly enables the direct measurements of stellar radii and effective temperatures further and further into the low-mass regime to provide comparison to stellar parameters derived by indirect methods, and indeed calibration of these methods themselves.

ACKNOWLEDGEMENTS

We thank the reviewer for the thorough analysis of the manuscript and helpful comments. We would furthermore like to express our sincere gratitude to Judit Sturmann for her tireless and invaluable support of observing operations at CHARA. Thanks to Sean Raymond, Barbara Rojas-Ayala, Phil Muirhead, Andrew Mann, Eric Gaidos and Lisa Kaltenegger for multiple insightful and useful discussions on various aspects of this work. TSB acknowledges support provided through NASA grant ADAP12-0172. The CHARA Array is funded by the National Science Foundation through NSF grants AST-0606958 and AST-0908253 and by Georgia State University through the College of Arts and Sciences, as well as the W. M. Keck Foundation. This research made use of the SIMBAD and VIZIER Astronomical Data bases, operated at CDS, Strasbourg, France (http://cdsweb.u-strasbg.fr/), and of NASA's Astrophysics Data System, of the Jean-Marie Mariotti Center `SearchCal` service (http://www.jmmc.fr/searchcal), co-developed by FIZEAU and LAOG/IPAG. This publication makes use of data products from the Two Micron All Sky Survey, which is a joint project of the University of Massachusetts and the Infrared Processing and Analysis Center/California Institute of Technology, funded by the National Aeronautics and Space Administration and the National Science Foundation. This research made use of the NASA Exoplanet Archive (Akeson et al. 2013), which is operated by the California Institute of Technology, under contract with the National Aeronautics and Space Administration under the Exoplanet Exploration Program. This work has made use of the HZ Gallery at hzgallery.org (Kane & Gelino 2012). This research has made use of the Exoplanet Orbit Database and the Exoplanet Data Explorer at exoplanets.org (Wright et al. 2011a). This research has made use of the Exoplanet Encyclopedia at exoplanet.eu (Schneider et al. 2011).

REFERENCES

Akeson R. L. et al., 2013, PASP, 125, 989
Allende Prieto C., Lambert D. L., 1999, A&A, 352, 555
Ammons S. M., Robinson S. E., Strader J., Laughlin G., Fischer D., Wolf A., 2006, ApJ, 638, 1004
Anderson E., Francis C., 2011, VizieR Online Data Catalog, 5137, 0
Anderson E., Francis C., 2012, Astron. Let., 38, 331
Argue A. N., 1963, MNRAS, 125, 557
Baines E. K., McAlister H. A., ten Brummelaar T. A., Turner N. H., Sturmann J., Sturmann L., Goldfinger P. J., Ridgway S. T., 2008a, ApJ, 680, 728
Baines E. K., McAlister H. A., ten Brummelaar T. A., Turner N. H., Sturmann J., Sturmann L., Ridgway S. T., 2008b, ApJ, 682, 577
Baines E. K., McAlister H. A., ten Brummelaar T. A., Sturmann J., Sturmann L., Turner N. H., Ridgway S. T., 2009, ApJ, 701, 154
Baines E. K. et al., 2010, AJ, 140, 167

Beichman C. A., Neugebauer G., Habing H. J., Clegg P. E., Chester T. J., eds, 1988, Infrared astronomical satellite (IRAS) catalogs and atlases. Volume 1: Explanatory supplement, Vol. 1
Bessel M. S., 1990, A&AS, 83, 357
Bessell M. S., 2000, PASP, 112, 961
Bonneau D. et al., 2006, A&A, 456, 789
Bonneau D., Delfosse X., Mourard D., Lafrasse S., Mella G., Cetre S., Clausse J. M., Zins G., 2011, A&A, 535, A53
Boyajian T. S. et al., 2012a, ApJ, 746, 101
Boyajian T. S. et al., 2012b, ApJ, 757, 112
Boyajian T. S. et al., 2013, ApJ, 771, 40
Bryden G. et al., 2009, ApJ, 705, 1226
Burnashev B. I., 1985, Bull. Crimean Astrophys. Obs., 66, 152
Butler R. P., Marcy G. W., Vogt S. S., Fischer D. A., Henry G. W., Laughlin G., Wright J. T., 2003, ApJ, 582, 455
Butler R. P. et al., 2006, ApJ, 646, 505
Casagrande L., Schönrich R., Asplund M., Cassisi S., Ramírez I., Meléndez J., Bensby T., Feltzing S., 2011, A&A, 530, A138
Cernis K., Meistas E., Straizys V., Jasevicius V., 1989, Vilnius Astron. Obser. Biuletenis, 84, 9
Claret A., 2000, A&A, 363, 1081
Clark J. P. A., McClure R. D., 1979, PASP, 91, 507
Correia A. C. M. et al., 2010, A&A, 511, A21
Cousins A. W. J., Stoy R. H., 1962, R. Greenwich Obs. Bull., 64, 103
Cutri R. M. et al., 2003, The 2MASS All Sky Catalog of Point Sources. IPAC, Pasadena
Dean J. F., 1981, South Afr. Astron. Obs. Circ., 6, 10
Demarque P., Woo J. H., Kim Y. C., Yi S. K., 2004, ApJS, 155, 667
Dodson-Robinson S. E., Beichman C. A., Carpenter J. M., Bryden G., 2011, AJ, 141, 11
Ecuvillon A., Israelian G., Santos N. C., Shchukina N. G., Mayor M., Rebolo R., 2006, A&A, 445, 633
Eiroa C. et al., 2013, A&A, 555, A11
Endl M., Cochran W. D., Wittenmyer R. A., Boss A. P., 2008, ApJ, 673, 1165
Erro B. I., 1971, Bol. Inst. Tonantzintla, 6, 143
Forveille T. et al., 2009, A&A, 493, 645
Fuhrmann K., Pfeiffer M. J., Bernkopf J., 1998, A&A, 336, 942
Galland F., Lagrange A. M., Udry S., Chelli A., Pepe F., Beuzit J. L., Mayor M., 2005, A&A, 444, L21
Gezari D. Y., Pitts P. S., Schmitz M., 1999, VizieR Online Data Catalog, 2225, 0
Glushneva I. N. et al., 1998, VizieR Online Data Catalog, 3207, 0
Golay M., 1972, Vistas Astron., 14, 13
Gonzalez G., Carlson M. K., Tobin R. W., 2010, MNRAS, 403, 1368
Gray R. O., Corbally C. J., Garrison R. F., McFadden M. T., Robinson P. E., 2003, AJ, 126, 2048
Häggkvist L., Oja T., 1966, Ark. Astron., 4, 137
Häggkvist L., Oja T., 1970, A&AS, 1, 199
Haggkvist L., Oja T., 1987, A&AS, 68, 259
Hanbury Brown R., Davis J., Lake R. J. W., Thompson R. J., 1974, MNRAS, 167, 475
Heiter U., Luck R. E., 2003, AJ, 126, 2015
Hekker S., Meléndez J., 2007, A&A, 475, 1003
Henry G. W. et al., 2013, ApJ, 768, 155
Holmberg J., Nordström B., Andersen J., 2009, A&A, 501, 941
Houdebine E. R., 2010, MNRAS, 407, 1657
Houdebine E. R., 2012, MNRAS, 421, 3189
Howard A. W. et al., 2009, ApJ, 696, 75
Huber D. et al., 2012, ApJ, 760, 32
Iriarte B., 1971, Bol. Obs. Tonantzintla Tacubaya, 6, 143
Jasevicius V., Kuriliene G., Strazdaite V., Kazlauskas A., Sleivyte J., Cernis K., 1990, Vilnius Astron. Obser. Biuletenis, 85, 50
Jenkins J. S., Ramsey L. W., Jones H. R. A., Pavlenko Y., Gallardo J., Barnes J. R., Pinfield D. J., 2009, ApJ, 704, 975
Johnson H. L., Knuckles C. F., 1957, ApJ, 126, 113
Johnson H. L., Mitchell R. I., 1975, Rev. Mex. Astron. Astrofis., 1, 299
Johnson H. L., Mitchell R. I., Iriarte B., Wisniewski W. Z., 1966, Commun. Lunar Planet. Lab., 4, 99
Johnson J. A. et al., 2007, ApJ, 665, 785
Johnson J. A. et al., 2010, PASP, 122, 149
Jones D. H. P., Sinclair J. E., Alexander J. B., 1981, MNRAS, 194, 403
Kane S. R., Gelino D. M., 2012, PASP, 124, 323
Kane S. R., Barclay T., Gelino D. M., 2013, ApJ, 770, L20
Kasting J. F., Whitmire D. P., Reynolds R. T., 1993, Icarus, 101, 108
Kazlauskas A., Boyle R. P., Philip A. G. D., Straižys V., Laugalys V., Černis K., Bartašiūtė S., Sperauskas J., 2005, Balt. Astron., 14, 465
Kervella P., Thévenin F., Morel P., Bordé P., Di Folco E., 2003, A&A, 408, 681
Kharitonov A. V., Tereshchenko V. M., Knjazeva L. N., 1988, The Spectrophotometric Catalogue of Stars. Nauka, Alma-Ata
Kilkenny D., Koen C., van Wyk F., Marang F., Cooper D., 2007, MNRAS, 380, 1261
Kim Y. C., Demarque P., Yi S. K., Alexander D. R., 2002, ApJS, 143, 499
Koen C., Kilkenny D., van Wyk F., Cooper D., Marang F., 2002, MNRAS, 334, 20
Koen C., Kilkenny D., van Wyk F., Marang F., 2010, MNRAS, 403, 1949
Koleva M., Vazdekis A., 2012, A&A, 538, A143
Kopparapu R. K. et al., 2013a, APJ, 765, 131
Kopparapu R. K. et al., 2013b, ApJ, 770, 82
Kornilov V. G. et al., 1991, Tr. Gos. Okeanogr. Inst., 63, 4
Kovtyukh V. V., Soubiran C., Belik S. I., 2004, A&A, 427, 933
Kozok J. R., 1985, A&AS, 61, 387
Lafrasse S., Mella G., Bonneau D., Duvert G., Delfosse X., Chelli A., 2010a, VizieR Online Data Catalog, 2300, 0
Lafrasse S., Mella G., Bonneau D., Duvert G., Delfosse X., Chesneau O., Chelli A., 2010b, in Danchi W. C., Delplancke F., Rajagopal J. K., eds, Proc. SPIE Conf. Ser. Vol. 7734, Optical and Infrared Interferometry II. SPIE, Bellingham, p. 77344E
Laughlin G., Butler R. P., Fischer D. A., Marcy G. W., Vogt S. S., Wolf A. S., 2005, ApJ, 622, 1182
Lawler S. M. et al., 2009, ApJ, 705, 89
Liu Y. J. et al., 2008, ApJ, 672, 553
Luck R. E., Heiter U., 2007, AJ, 133, 2464
McWilliam A., 1990, ApJS, 74, 1075
McClure R. D., Forrester W. T., 1981, Publ. Dom. Astrophys. Obs. Vic., 15, 439
Maldonado J., Villaver E., Eiroa C., 2013, A&A, 554, A84
Manteiga M., Carricajo I., Rodríguez A., Dafonte C., Arcay B., 2009, AJ, 137, 3245
Markwardt C. B., 2009, in Bohlender D. A., Durand D., Dowler P., eds, ASP Conf. Ser. Vol. 411, Astronomical Data Analysis Software and Systems XVIII. Astron. Soc. Pac., San Francisco, p. 251
Marsakov V. A., Shevelev Y. G., 1995, Bull. Inf. Cent. Donnees Stellaires, 47, 13
Mayor M. et al., 2011, preprint (arXiv:e-prints)
Mermilliod J. C., 1986, Catalogue of Eggen's UBV data, 0, 0
Mishenina T. V., Soubiran C., Bienaymé O., Korotin S. A., Belik S. I., Usenko I. A., Kovtyukh V. V., 2008, A&A, 489, 923
Mishenina T. V., Soubiran C., Kovtyukh V. V., Katsova M. M., Livshits M. A., 2012, A&A, 547, A106
Morales J. C., Ribas I., Jordi C., 2008, A&A, 478, 507
Mould J. R., Hyland A. R., 1976, ApJ, 208, 399
Mumford G. S., 1956, AJ, 61, 213
Noyes R. W., Jha S., Korzennik S. G., Krockenberger M., Nisenson P., Brown T. M., Kennelly E. J., Horner S. D., 1997, ApJ, 483, L111
Oja T., 1996, Balt. Astron., 5, 103
Olsen E. H., 1994, A&AS, 106, 257
Olson E. C., 1974, AJ, 79, 1424
Persson S. E., Aaronson M., Frogel J. A., 1977, AJ, 82, 729
Petigura E. A., Marcy G. W., 2011, ApJ, 735, 41
Pickles A. J., 1998, PASP, 110, 863
Prugniel P., Vauglin I., Koleva M., 2011, A&A, 531, A165
Ramírez I., Meléndez J., 2005, ApJ, 626, 465

Rivera E. J., Butler R. P., Vogt S. S., Laughlin G., Henry G. W., Meschiari S., 2010a, ApJ, 708, 1492
Rivera E. J., Laughlin G., Butler R. P., Vogt S. S., Haghighipour N., Meschiari S., 2010b, ApJ, 719, 890
Rojas-Ayala B., Covey K. R., Muirhead P. S., Lloyd J. P., 2012, ApJ, 748, 93
Sanders W. L., 1966, AJ, 71, 719
Schiavon R. P., 2007, ApJS, 171, 146
Schneider J., Dedieu C., Le Sidaner P., Savalle R., Zolotukhin I., 2011, A&A, 532, A79
Schröder C., Reiners A., Schmitt J. H. M. M., 2009, A&A, 493, 1099
Selsis F., Kasting J. F., Levrard B., Paillet J., Ribas I., Delfosse X., 2007, A&A, 476, 1373
Skiff B. A., 1994, Inf. Bull. Var. Stars, 3984, 1
Soubiran C., Le Campion J. F., Cayrel de Strobel G., Caillo A., 2010, A&A, 515, A111
Sperauskas J., Bartkevicius A., Zdanavicius K., 1981, Vilnius Astron. Obser. Biuletenis, 58, 3
Stauffer J. R., Hartmann L. W., 1986, ApJS, 61, 531
Straizys V., 1970, Dissertation thesis, Vilnius Univ., Lithuania
Takeda Y., 2007, PASJ, 59, 335
Takeda G., Ford E. B., Sills A., Rasio F. A., Fischer D. A., Valenti J. A., 2007, ApJS, 168, 297
Tanner A., Beichman C., Bryden G., Lisse C., Lawler S., 2009, ApJ, 704, 109
ten Brummelaar T. A. et al., 2005, ApJ, 628, 453
The P. S., Steenman H. C., Alcaino G., 1984, A&A, 132, 385
Trilling D. E. et al., 2008, ApJ, 674, 1086
Valdes F., Gupta R., Rose J. A., Singh H. P., Bell D. J., 2004, ApJS, 152, 251
Valenti J. A., Fischer D. A., 2005, ApJS, 159, 141
van Belle G. T., van Belle G., 2005, PASP, 117, 1263
van Belle G. T., von Braun K., 2009, ApJ, 694, 1085
van Leeuwen F., 2007, in Gerhard B., eds, Astrophysics and Space Science Library, Vol. 350, Hipparcos, the New Reduction of the Raw Data. Springer, Berlin, p. 20
Vogt S. S. et al., 2010, ApJ, 708, 1366
von Braun K. et al., 2011a, ApJ, 729, L26
von Braun K. et al., 2011b, ApJ, 740, 49
von Braun K. et al., 2012, ApJ, 753, 171
Weis E. W., 1984, ApJS, 55, 289
Weis E. W., 1986, AJ, 91, 626
Weis E. W., 1987, AJ, 93, 451
Weis E. W., 1993, AJ, 105, 1962
Weis E. W., 1996, AJ, 112, 2300
Weis E. W., Upgren A. R., 1982, PASP, 94, 821
Wright C. O., Egan M. P., Kraemer K. E., Price S. D., 2003, AJ, 125, 359
Wright J. T. et al., 2011a, PASP, 123, 412
Wright N. J., Drake J. J., Mamajek E. E., Henry G. W., 2011b, ApJ, 743, 48
Wu Y., Singh H. P., Prugniel P., Gupta R., Koleva M., 2011, A&A, 525, A71
Yi S., Demarque P., Kim Y. C., Lee Y. W., Ree C. H., Lejeune T., Barnes S., 2001, ApJS, 136, 417
Yoss K. M., Griffin R. F., 1997, J. Astrophys. Astron., 18, 161
Zakhozhaj V. A., 1979, Vestn. Khar'k. Univ., 190, 52

This paper has been typeset from a TEX/LATEX file prepared by the author.